Multifractal Products of Stochastic Processes: Fluid Flow Analysis

Patrik Carlsson and Markus Fiedler
University of Karlskrona/Ronneby
Dept. of Telecommunications and Signal Processing
S-371 79 Karlskrona
{Patrik.Carlsson,Markus.Fiedler}@its.hk-r.se

Abstract

The consideration of multifractal properties in network traffic has become a well-known issue in network performance evaluation. We analyze the performance of a fluid flow buffer fed by multifractal traffic described by Norros, Mannersalo and Riedi [1]. We describe specific steps in fluid flow analysis, both for finite and infinite buffer sizes, and point out how to overcome numerical problems. We discuss performance results in form of waiting time quantiles and loss probabilities, which help to estimate whether a traffic concentrator constitutes a bottleneck or not.

Keywords: Multifractal traffic, fluid flow model, numerical analysis, performance evaluation

1 Introduction

It has been demonstrated that teletraffic exhibits multifractal properties [1]. However, there is still a lack of performance models that allows for taking such behavior into account. In our study we take a step towards closing that gap by applying fluid flow analysis to a specific process with multifractal properties. Mannersalo, Norros and Riedi [1] proposed a traffic model that exhibits such multifractal properties: *In its simplest form our model is based on the multiplication of independent rescaled stochastic processes* $\Lambda^{(i)}(\cdot) \stackrel{\mathrm{d}}{=} \Lambda(b^i \cdot)$ *which are piecewise constant. ... In multiplying rather than adding re-scaled versions of a 'mother' process we obtain a process with novel properties which are best understood not in an additive analysis, but in a multiplicative one. Moreover, processes emerging from multiplicative construction ... exhibit typically a 'spiky' appearance* [1]. The 'mother'- or base process is a Markov-modulated rate processes (MMRP) with two activity states, which is well-known in fluid flow analysis. But in contrast to the commonly used additive superposition of the data rates of the MMRPs, the contributions of the subprocesses that act on different time scales to the total data rate are multiplied together. Thus, with exception of some decomposition results [2], fluid flow analysis can be used straightforward.

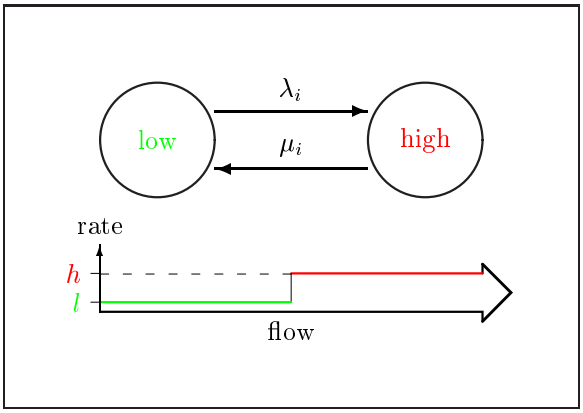

Figure 1. State diagram for one subprocess.

Mannersalo, Norros and Riedi left queuing experiments for further study [1]. This paper is a continuation of their work. It is organized as follows: Section 2 describes the multifractal products of stochastic processes. Section 3 deals with the corresponding fluid flow analysis; it describes how to create the basic matrices and how to avoid numerical problems. Section 4 presents performance results for two such processes in terms of waiting time quantiles and loss probabilities. Such results help to estimate to which extent, for a given input process and load of outgoing link, the concentrator acts as a bottleneck. Section 5 contains a summary and open issues. The appendix shows an example of matrices for the fluid flow analysis.

2 Multifractal Products of Stochastic Processes

Our study and [1] are based on the same data generation process. The outputs of independent subprocesses are multiplied together,

$$R(t) = \prod_{i=0}^{n-1} R_i(t)\,, \tag{1}$$

while the familiy of subprocesses is given by

$$R_i(t) = R_0(b^i t)\,,\ b > 1\,. \tag{2}$$

For $n \to \infty$, an "asymptotically self-similar" process is obtained [1].

The only difference between the subprocesses is their time scale: Compared to process 0, process i is slowed down by factor b^i. As subprocess, a 2-state Markov-modulated rate process (MMRP) with a Markov chain as depicted in Figure 1 is used. With (2), the transition rates of subprocess i become

$$\lambda_i = b^{-i}\lambda_0\,, \tag{3}$$

$$\mu_i = b^{-i}\mu_0\,. \tag{4}$$

Process	MNR	SYM
l_i	$1/3$	$1/2$
h_i	$7/6$	$3/2$
λ_i	$5/4^i$	$2/4^i$
μ_i	$5/4^{i+1}$	$2/4^i$
b	4	4
n	7	7

Table 1. Summary of process parameters.

We assume that data and time units are chosen such that on average, one data unit is produced during one time unit [1]:

$$\mathbf{E}[R] = \mathbf{E}\left[\prod_{i=0}^{n-1} R_i\right] \equiv 1 \quad \forall n\,. \tag{5}$$

In the following, data and transitions rates as well as times and buffer-related sizes are given in these units without explicitly referring to them. Accordingly, λ_i and μ_i are chosen such that

$$\mathbf{E}[R_i] = \frac{\mu_i l_i + \lambda_i h_i}{\mu_i + \lambda_i} \equiv 1 \quad \forall i\,, \tag{6}$$

$$\tau_0 = \frac{1}{\lambda_0} + \frac{1}{\mu_0}\,, \tag{7}$$

which means that the mean cycle time of the slowest subprocess becomes the time unit. This leads to the mean cycle time of subprocess i

$$\tau_i = b^i\,. \tag{8}$$

We use two processes in our study.

1. *MNR process*: a process specified by Mannersalo, Norros and Riedi [1], but re-scaled in time to meet (7).
2. *SYM process*: a process with symmetric transition rates ($\lambda_i \equiv \mu_i$).

The parameters of the processes are shown in Table 1.

Let $n(t,T)$ be the mean number of data units that are produced by $R(t)$ during the time interval $]t-T, T]$:

$$n(t,T) = \int_{t-T}^{t} R(t)\mathrm{d}t\,. \tag{9}$$

Plots of $n(t,T)$ for the MNR process and different time scales T are shown in Figure 2 and reveal multifractal behavior. For $T = 1$ and $T = 100$, the variations of $n(t,T)$ the process around its expectation T nearly look the same. For $T = 10000$, which is larger than the mean cycle time of the slowest sub-process $\tau^6 = 4096$, the variations

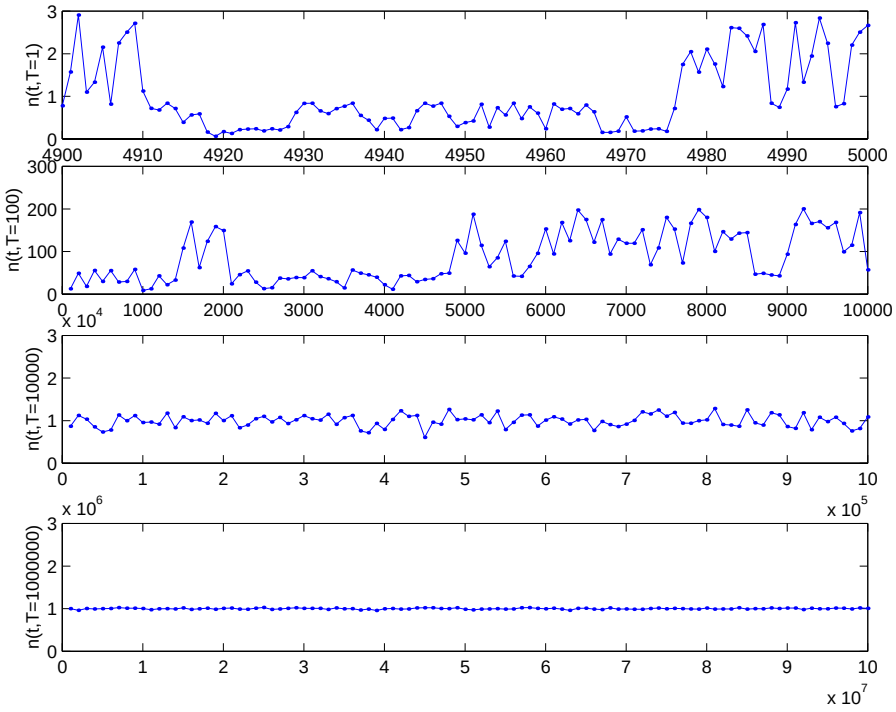

Figure 2. Mean number of data units vs. time for different time intervals T, MNR process.

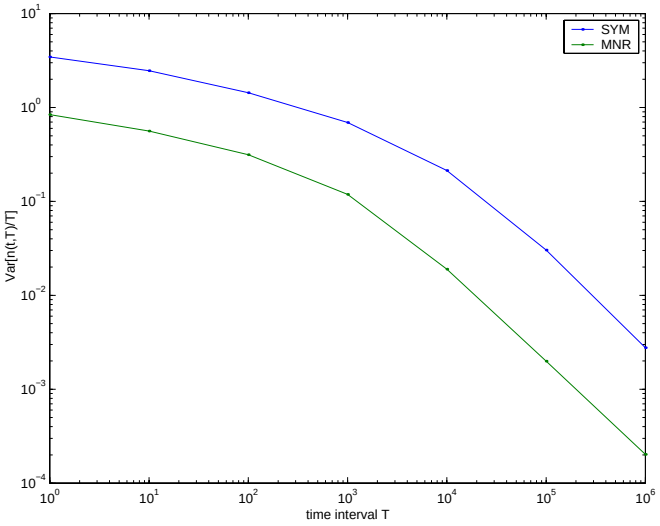

Figure 3. Variance time plots for the MNR and SYM process.

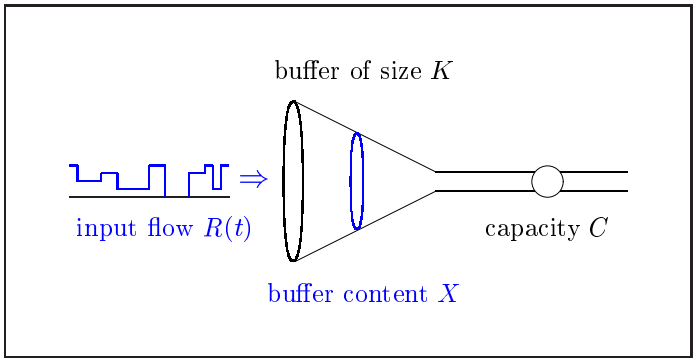

Figure 4. Fluid flow model of a concentrator.

become less, and for $T = 1000000$, they have almost disappeared. This behavior is underlined by the variance-time plot shown in Figure 3. It shows two distinctive parts for both MNR and SYM process: The normalized variance $\mathbf{Var}[n(t,T)/T] \sim T^{\beta+1}$ [3] decays more quickly on long time scales than on short ones (*cf.* figures shown in [4]). On short time scales ($T = 1 \ldots 100$), a simple least-square approximation gives an estimate $\hat{\beta} \simeq -1.50/-1.44$ for the MNR/SYM process, while on long time scales ($T = 10^5 \ldots 10^6$), $\hat{\beta} \simeq -2$, which means short-range dependence. This is due to the choice of b and n, the latter of which has to be finite in order to make analysis possible. At this stage, the investigation of the role of these parameters is left for further study.

3 Fluid Flow Analysis

The analysis of the fluid flow model is based on two matrices, the transition rate matrix $\mathbf{M}$ and the diagonal drift matrix $\mathbf{D}$, whose elements d_s show how the buffer content behaves if the process is in a particular state s:

- Positive drift $d_s > 0$: the buffer content rises until the buffer overflows; s is an *overload state*.
- Vanishing drift $d_s = 0$: the buffer content remains unchanged.
- Negative drift $d_s < 0$: the buffer content sinks until the buffer becomes empty; s is an *underload state*.

The construction of these matrices is discussed in Section 3.1.

The fluid flow model of a concentrator is shown in Figure 4. We assume a constant capacity C; the offered load becomes

$$A = \frac{\mathbf{E}[R]}{C} = \frac{1}{C}\,. \tag{10}$$

The behavior of the buffer content of the concentrator

$$\vec{F}^T(x) = [F_0(x)\, F_1(x) \ldots F_N(x)]\,, \tag{11}$$

with

$$F_n(x) = \Pr\{\text{state } S = n, X \leq x\} \,, \tag{12}$$

is given by the set of differential equations

$$\mathbf{D}\frac{\mathrm{d}\vec{F}(x)}{\mathrm{d}x} = \mathbf{M}\vec{F}(x)\,, \quad 0 \leq x < K\,. \tag{13}$$

The boundary conditions are

$$F_n(0) = 0 \qquad d_n > 0 \tag{14}$$

$$F_n(K) = \Pr\{S = n\} = \pi_n \qquad d_n < 0 \tag{15}$$

The solution is given by:

$$\vec{F}(x) = \sum a_q \phi_q e^{z_q x}\,, \tag{16}$$

where z_q and ϕ_q are the eigenvalues and corresponding eigenvectors found through

$$z_q\phi_q = \mathbf{D}^{-1}\mathbf{M}\phi_q\,. \tag{17}$$

We normalize the eigenvectors to a component sum of one. Vanishing drift values have to be excluded so that $\mathbf{D}$ is invertible, which leads to the condition

$$\{l^{n-i}h^i\} \neq C \quad i = 0 \ldots n\,. \tag{18}$$

The coefficients a_q are obtained from solving the linear system of equations given by (14), and (15) in case of buffers of finite size. For *buffers of infinite size* $K \to \infty$, merely coefficients belonging to negative eigenvalues have to be determined, as besides of $a_0 = 1$ for $z_0 = 0$ and $\Phi_0 = \vec{\pi}$ (the vector of state probabilities), all other coefficients belonging to positive eigenvalues have to disappear [5]. In this case, the *complementary probability distribution function* (cpdf) of a buffer threshold x is given by

$$G(x) = \Pr\{X > x\} = -\sum_{q:z_q<0} a_q e^{z_q x}\,. \tag{19}$$

Instead of x, a waiting time threshold $w = x/C$ can serve as analysis parameter. For *buffers of finite size*, the loss probability is calculated through [6]:

$$P_{\text{Loss}} = \frac{1}{\mathbf{E}[R]} \sum_{\forall S:d_s>0} \left(\Pr\{S = s\} - F_s(K^-)\right) d_s\,. \tag{20}$$

A detailed description of fluid flow analysis is contained in [7, 8].

3.1 Matrix construction

The matrices $\mathbf{M}$ and $\mathbf{R}$ used in fluid flow analysis are constructed from the matrices of the subprocesses

$$\mathbf{M}_i = \begin{bmatrix} -\lambda_i & \lambda_i \\ \mu_i & -\mu_i \end{bmatrix} = \begin{bmatrix} -b^{-i}\lambda_0 & b^{-i}\lambda_0 \\ b^{-i}\mu_i & -b^{-i}\mu_i \end{bmatrix}, \tag{21}$$

$$\mathbf{R}_i = \begin{bmatrix} l & 0 \\ 0 & h \end{bmatrix}. \tag{22}$$

The transition rate matrix is formed using Kronecker addition [2]

$$\mathbf{M} = \mathbf{M}_0 \oplus \mathbf{M}_1 \oplus \cdots \oplus \mathbf{M}_{n-1}. \tag{23}$$

The rate matrix is constructed slightly different from the ordinary case where the sources data rates are added to each other. Instead the diagonal of $\mathbf{R}$ is formed by multiplying each subprocess contribution to that particular state:

$$\mathbf{R} = \begin{bmatrix} l^n & 0 & 0 & 0 & \dots & 0 \\ 0 & l^{n-1}h & 0 & 0 & \dots & 0 \\ 0 & 0 & l^{n-2}hl & 0 & \dots & 0 \\ 0 & 0 & 0 & l^{n-2}h^2 & \dots & 0 \\ \dots & \dots & \dots & \dots & \dots & \\ 0 & 0 & 0 & 0 & \dots & h^n \end{bmatrix}. \tag{24}$$

The drift matrix $\mathbf{D}$ is formed as usually through

$$\mathbf{D} = \mathbf{R} - C\mathbf{I} \tag{25}$$

In the Appendix A, a simple example is given. In general the matrices will be of size $[2^n \times 2^n]$, i.e. a large system appears even for quite small values of n. The matrices are irreducible due to the fact that all the subprocesses have different transition rates.

3.2 Resolving numerical problems

Underload states with drift values near to zero lead to very large positive eigenvalues that may cause numerical overflow in (15). However, previous numerical studies [7, 9] revealed that the corresponding coefficient became extremely small as the drift approached zero from below, so that the contribution of the corresponding term to (16) vanishes. Consequently and with respect to the limit of about 10^{308} (imposed by floating-points with double precision), coefficients a_q for eigenvalues that would lead to

$$e^{z_q K} > 10^{300} \tag{26}$$

were set to zero in advance, and the same number of equations (belonging to states with smallest negative drifts) were removed before solving the system of equations.

The numerical calculations were performed using MATLAB™. The eigensystem was calculated by a routine from the NAG® Foundation toolbox, while the coefficients were obtained through a standard matrix inversion. The improvement of the numerical behavior for larger n is left for further study.

A	C	a_η	z_η
80 %	1.25	-0.71830	-0.0020215
70 %	1.41	-0.59157	-0.0064305
60 %	1.67	-0.47322	-0.022768
50 %	2.00	-0.36367	-0.10132
40 %	2.50	-0.26401	-0.76108
30 %	3.33	0	—

Table 2. Coefficients and eigenvalues for different loads for the MNR process and infinite buffer.

4 Results

First, we take a look at the *MNR process* (for parameters, see Table 1) in conjunction with a buffer of infinite size. As the offered load is bounded by $A < 1$, this process has only one overload state when $R(t) = h^7 \simeq 2.9419$. Thus, there will only be one negative eigenvalue z_η; the corresponding coefficient is denoted by a_η. Consequently, the cpdf of the waiting time is given by a simple exponential:

$$G(w) = \Pr\{W > w\} = -a_\eta e^{z_\eta C w}\,. \tag{27}$$

Some selected eigenvalues z_η and coefficients a_η are shown in Table 2. For a load of 30 %, no overload ever happens due to the fact that $C > h^7$, which means that the buffer always remains empty. However, as the link load increases beyond 50 %, given the same input traffic pattern, the concentrator turns into a bottleneck. The critical value is not the coefficient, but the eigenvalue contained in the exponential term that diminishes rapidly with rising load, thus pushing up the tail of the cpdf. This is illustrated by Figure 5. Especially for a load of 70–80 %, the curves decay very slowly, indicating that very heavy queuing will occur. These results are underlined by the *waiting time quantiles* $w_k : G(w_k) = \Pr\{W > w_k\} = 10^{-k}$ given by

$$w_k = A\,\frac{k\ln(10) + \ln(a_\eta(A))}{|z_\eta(A)|}\,. \tag{28}$$

These quantiles grow linearly with the desired level k, while according to Table 2, the load mostly affects the eigenvalue in the denominator. Figure 6 reveals that waiting time quantiles approximately rise exponentially with the load.

Figure 7 shows the corresponding loss probabilities in a buffer of finite size K that bounds the *maximal waiting time* to $w_{\max} = K/C$. These loss probabilities exhibit similar exponential tails as the corresponding cpdf's. For this process, a load of 40–50 % implies good loss performance even for quite small buffer sizes. In case of high loads, the concentrator with a buffer of finite size throws away a considerable share of the input traffic.

Finally we turn to the *SYM process*. The cpdf of the waiting time is shown in Figure 8. A comparison with the corresponding cpdf of the MNR process (Figure 5) reveals that queuing has become heavier, which was to be expected from the greater

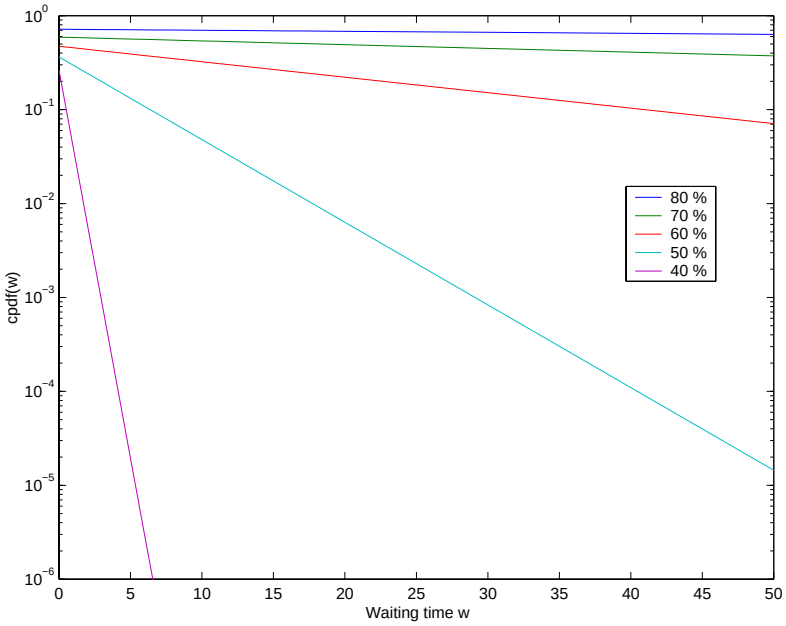

Figure 5. Complementary waiting time distribution for different offered loads, MNR process.

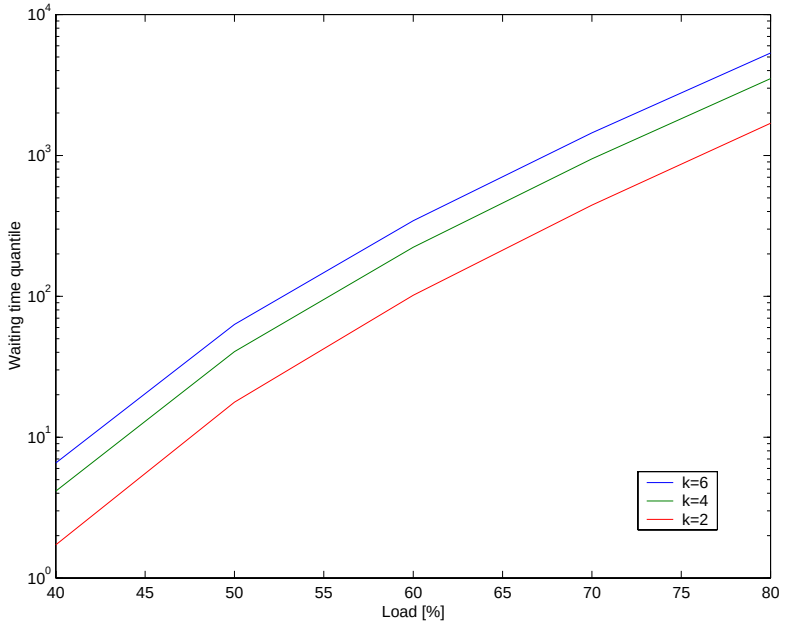

Figure 6. Waiting time quantiles for different levels, MNR process.

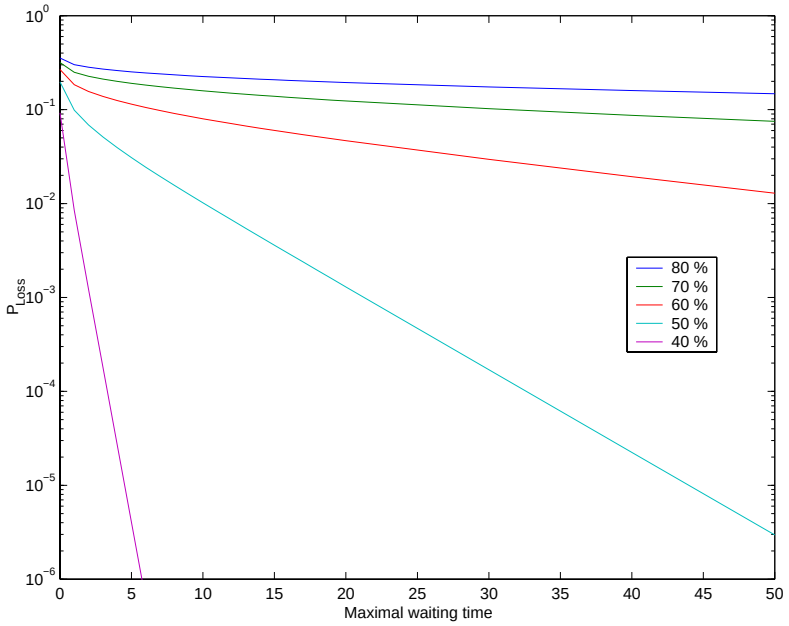

Figure 7. Loss probability vs. maximal waiting time for different offered loads, MNR process.

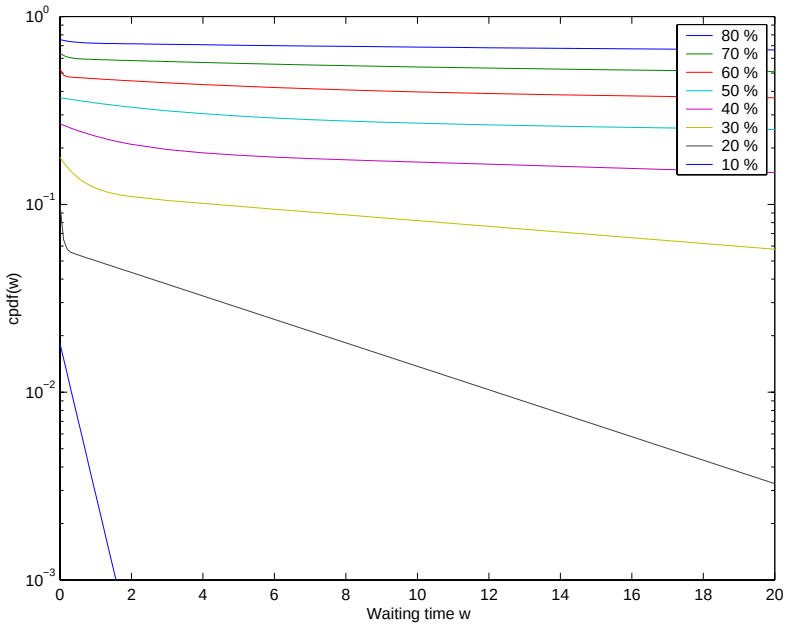

Figure 8. Complementary waiting time distribution for different offered loads, SYM process.

A	C	Negative eigenvalues	
		number	set
10 %	10.00	1	{-0.18477}
20 %	5.00	9	{-0.028764, -3.3645 ... -3.946}
60 %	1.67	28	{-0.0017248, -0.086306 ... -0.75685, -11.838 ... -11.907 }

Table 3. Eigenvalues, SYM process. The dominant eigenvalues are underlined.

variance of the SYM process, see Figure 3. If the concentrator were loaded by more than 20 %, it would probably become a bottleneck.

Even though the cpdf contains more than one exponential term, except from the case with 10 % load, an exponential tail occurs due to the dominance of the negative eigenvalue with the smallest absolute value, see Table 3.

5 Conclusions

In this paper, we presented a fluid flow queuing experiment for a process with multifractal properties specified by Mannersalo, Norros and Riedi [1]. We discussed main steps in fluid flow analysis of a traffic concentrator as well as related numerical issues and presented results for waiting time quantiles and loss probabilities. Such results might be used for estimating whether a concentrator constitutes a bottleneck, given an input process with multifractal properties and a certain load of the outgoing link. Thus, the use of multifractal products of processes together with the fluid flow model seems to be a promising way of analyzing network traffic.

However, we had to leave some important issues for further study. One of them is to study the impact of the process parameters in detail. As stated by [1], modeling of real traffic should be taken into account, which makes it necessary to develop parameter estimators and synthesis algorithms for matching real data traffic. Finally, possibilities to stabilize the fluid flow calculations for very large systems, i.e. many contributing subprocesses, should be investigated.

References

[1] P. Mannersalo, I. Norros, and R. Riedi. Multifractal products of stochastic processes: A preview. *COST-257 Technical Document* 257TD(99)31. `http://nero.informatik.uni-wuerzburg.de/cost/Final/TDs/257td9931.pdf`

[2] T.E. Stern and A. Elwalid. Analysis of separable markov-modulated rate models for information-handling systems. *Advances in Applied Probability*, 23:105-139 (1991).

[3] I. Norros. On the use of fractional brownian motion in the theory of connectionless networks. *IEEE Journal on Selected Areas in Communications*, 13(6):953-962 (1995).

[4] A. Veres, Zs. Kenesi, S. Molnár, and G. Vattay. On the propagation of long-range dependence in the Internet. *To be presented at ACM SIGCOMM 2000*, Stockholm, Sweden, August 2000.

[5] D. Anick, D. Mitra, M.M. Sondhi. Stochastic theory of a data-handling system with multiple sources. *The Bell System Technical Journal*, 61(8):1871–1894 (1982).

[6] R. Tucker. Accurate method for analysis of a packet-speech multiplexer with limited delay. *IEEE Transactions on Communications*, 36(4):479–483 (1988).

[7] M. Fiedler and H. Voos. How to win the numerical battle against the finite buffer stochastic fluid flow model. *COST-257 Technical Document* 257TD(99)38. `http://nero.informatik.uni-wuerzburg.de/cost/Final/TDs/257td9938.pdf`

[8] M. Fiedler. Modeling and analysis of wireless network segments with the aid of teletraffic fluid flow models. *Research report 5/00. University of Karlskrona/Ronneby*, Sweden, ISSN 1103 1581.

[9] M. Fiedler and H. Voos. Fluid flow-Modellierung von ATM-Multiplexern. Mathematische Grundlagen und numerische Lösungsmethoden. München: Utz, 1997, ISBN 3-89675-251-0.

A Example of matrix construction

The following matrices belong to a process with $\lambda_0 = \mu_0 = 2$, $l = 0.5$, $h = 1.5$, $b = 4$ and $n = 3$. Observe the exponential growth of data rates in matrix $\mathbf{R}$.

$$\mathbf{M}_0 = \begin{bmatrix} -2 & 2 \\ 2 & -2 \end{bmatrix} \qquad \mathbf{M}_1 = \begin{bmatrix} -0.5 & 0.5 \\ 0.5 & -0.5 \end{bmatrix} \qquad \mathbf{M}_2 = \begin{bmatrix} -0.125 & 0.125 \\ 0.125 & -0.125 \end{bmatrix}$$

$$\mathbf{R}_0 = \begin{bmatrix} 0.5 & 0 \\ 0 & 1.5 \end{bmatrix} \qquad \mathbf{R}_1 = \begin{bmatrix} 0.5 & 0 \\ 0 & 1.5 \end{bmatrix} \qquad \mathbf{R}_2 = \begin{bmatrix} 0.5 & 0 \\ 0 & 1.5 \end{bmatrix}$$

$$\mathbf{M} = \begin{bmatrix} -2.625 & 0.125 & 0.5 & 0 & 2 & 0 & 0 & 0 \\ 0.125 & -2.625 & 0 & 0.5 & 0 & 2 & 0 & 0 \\ 0.5 & 0 & -2.625 & 0.125 & 0 & 0 & 2 & 0 \\ 0 & 0.5 & 0.125 & -2.625 & 0 & 0 & 0 & 2 \\ 2 & 0 & 0 & 0 & -2.625 & 0.125 & 0.5 & 0 \\ 0 & 2 & 0 & 0 & 0.125 & -2.625 & 0 & 0.5 \\ 0 & 0 & 2 & 0 & 0.5 & 0 & -2.625 & 0.125 \\ 0 & 0 & 0 & 2 & 0 & 0.5 & 0.125 & -2.625 \end{bmatrix}$$

$$\mathbf{R} = \begin{bmatrix} 0.125 & 0 & 0 & 0 & 0 & 0 & 0 & 0 \\ 0 & 0.375 & 0 & 0 & 0 & 0 & 0 & 0 \\ 0 & 0 & 0.375 & 0 & 0 & 0 & 0 & 0 \\ 0 & 0 & 0 & 1.125 & 0 & 0 & 0 & 0 \\ 0 & 0 & 0 & 0 & 0.375 & 0 & 0 & 0 \\ 0 & 0 & 0 & 0 & 0 & 1.125 & 0 & 0 \\ 0 & 0 & 0 & 0 & 0 & 0 & 1.125 & 0 \\ 0 & 0 & 0 & 0 & 0 & 0 & 0 & 3.375 \end{bmatrix}$$